Conditional deletion of β1 integrins in the intestinal epithelium causes a loss of Hedgehog expression, intestinal hyperplasia, and early postnatal lethality

Robert G. Jones,[1,3,4] Xiufen Li,[1,4] Phillip D. Gray,[1,4] Jinqiu Kuang,[1,4] Frederic Clayton,[2,4] Wade S. Samowitz,[2] Blair B. Madison,[5] Deborah L. Gumucio,[5] and Scott K. Kuwada[1,3,4]

[1]Huntsman Cancer Institute, [2]Department of Pathology, and [3]Department of Medicine, University of Utah, Salt Lake City, UT 84112
[4]Salt Lake City Veterans Administration Health Care System, Salt Lake City, UT 84112
[5]Deptartment of Cell and Developmental Biology, University of Michigan, Ann Arbor, MI 48109

Conditional deletion of β1 integrins in the intestinal epithelium, unlike in epidermal and mammary epithelia, of mice does not result in decreased cell adhesion and proliferation, but instead causes a profound increase in epithelial proliferation with dysplasia and polypoid structures. The increased epithelial proliferation inhibited epithelial differentiation that caused severe malnutrition and early postnatal lethality. The striking similarities between β1 integrin–deleted mice and neonatal mice with defective Hedgehog signaling led to the discovery that Hedgehog expression was markedly reduced in the former mice. β1 integrins were found to drive the expression of Hedgehogs in intestinal epithelial cells in an HNF-3β (*Foxa2*)–dependent fashion. The expression of Tcf-4, a transcription factor known to be required for intestinal epithelial stem cell proliferation, was increased and mislocalized in the intestinal epithelia of the β1 integrin–deleted mice and in newborn mice treated with the Hedgehog signaling inhibitor cyclopamine. This study shows that β1 integrins are key regulators of proliferation and homeostasis in the intestine and achieve this not through anchorage-dependent effects but by generating Hh expression and signaling.

Introduction

In epithelial cells, autocrine growth factor signaling requires coordinate input from β1 integrins for cell cycle progression (Clark and Brugge, 1995; Zhu and Assoian, 1995; Wary et al., 1996, 1998; Schwartz and Baron, 1999). Conditional deletion of β1 integrins in skin and mammary epithelia confirmed the dependence of proliferation in these tissues on β1 integrin–mediated cell adhesion in vivo (Brakebusch et al., 2000; Raghavan et al., 2000; Faraldo et al., 2001). However, the role of β1 integrins in the regulation of epithelial cell proliferation in vivo has only been tested in a limited number of tissues.

Within the digestive tract, the intestinal epithelial cells (IECs) express several α/β1 integrin heterodimers that mediate binding to ECM proteins (Beaulieu et al., 1991; Beaulieu, 1992; Fujimoto et al., 2002) and mediate adhesion to the underlying basement membrane. During late embryogenesis and the early postnatal period, the intestine becomes highly compartmentalized, which leads to the formation of the crypts of Lieberkühn and villi. The villi greatly increase the surface area for nutrient absorption and are generated by the stroma (mesodermal origin), which pushes the overlying IECs (endoderm origin) into the gut lumen. Stem cells take up residence near the bottoms of the crypts and give rise to four lineages of IECs (absorptive/enterocytic, enteroendocrine, goblet, and Paneth) that, with the exception of Paneth cells, migrate up the villi, differentiate, and are sloughed off within 3–5 d (Potten and Loeffler, 1990). Over 90% of the IECs are absorptive enterocytes.

The huge turnover of IECs requires vigorous intestinal crypt proliferation, which is mediated by key growth factor signaling pathways. Wnt signaling is a major driving force behind IEC proliferation (Pinto et al., 2003; Kuhnert et al., 2004), whereas Hh and Bmp signaling normally inhibit IEC proliferation (Howe et al., 1998, 2001; Woodford-Richens et al., 2000; Zhou et al., 2001; Abbi et al., 2002). The role of ECM–integrin interactions in the regulation of intestinal epithelial proliferation

Correspondence to Scott K. Kuwada: scott.kuwada@hsc.utah.edu

Abbreviations used in this paper: ERK, extracellular signal–regulated kinase; G3PDH, glyceraldehyde-3-phosphate dehydrogenase; IEC, intestinal epithelial cell; NHE3, sodium hydrogen exchanger 3; P, postnatal day; RIE, rat intestinal epithelial.

The online version of this article contains supplemental material.

The Journal of Cell Biology, Vol. 175, No. 3, November 6, 2006 505–514
http://www.jcb.org/cgi/doi/10.1083/jcb.200602160

through these or other growth factor signaling pathways in vivo is not well understood.

Some of the epithelial α/β1 integrin heterodimers and the ECM proteins within the basement membrane that they bind are expressed in gradients along the crypt–villous axis, as are various growth factors and their cognate receptors, and may provide important positional cues for the IECs (Beaulieu et al., 1991; Kedinger et al., 1998; Fujimoto et al., 2002). Although the intestinal epithelial stem cells comprise a subset of the β1 integrin–expressing IECs (Fujimoto et al., 2002; Dekaney et al., 2005), the role β1 integrins in intestinal epithelial proliferation has not been tested in vivo. We have used a conditional gene deletion system to determine the role of β1 integrins in intestinal epithelial proliferation.

Results

Mice carrying *Villin-Cre* (Madison et al., 2002) and *Itgb1*^{flox} (Raghavan et al., 2000) transgenes (Fig. 1, A and B) were crossed to generate *villin-Cre/Itgb1*$^{flox/flox}$ mice. Intestinal epithelial–specific recombination of the loxP sites was confirmed by PCR (Fig. 1 C), and loss of β1 integrin protein expression was verified by immunodetection (Fig. 1 D and Fig. S1, A and B, available at http://www.jcb.org/cgi/content/full/jcb.200602160/DC1). Consistent with previous results, Cre-mediated recombination was detected by PCR only in genomic DNA isolated from the small intestine and the proximal large intestine, but not from the stomach or kidneys (Fig. 1 C; Madison et al., 2002).

Villin-Cre/Itgb1$^{flox/flox}$ mouse pups were born at the expected frequencies. At embryonic day 18 and birth, the appearance and size of the pups and intestinal organs were similar in all littermates (unpublished data). However, by postnatal day (P) 4, the *villin-Cre/Itgb1*$^{flox/flox}$ mice were less than half the body weight of their control littermates (*villin-Cre/Itgb1*$^{flox/+}$ or *Itgb1*$^{flox/flox}$; Fig. 1, E and F) and died between P7 and P14 from severe malnutrition. The early deaths were not due to a lack of feeding, as the stomachs of all the newborn mice were full of colostrum at the time of death (unpublished data).

The intestinal epithelium not only carries out nutrient absorption but also presents a barrier to the environment. Because of previous reports that β1 integrins mediate IEC survival ex vivo (Strater et al., 1996), the *villin-Cre/Itgb1*$^{flox/flox}$ mice were carefully examined for evidence of mucosal defects resulting from a loss of IECs. Cleaved caspase 3 immunohistochemistry revealed the presence of rare apoptotic IECs in the *villin-Cre/Itgb1*$^{flox/flox}$ mice and control littermates, but the prevalence of

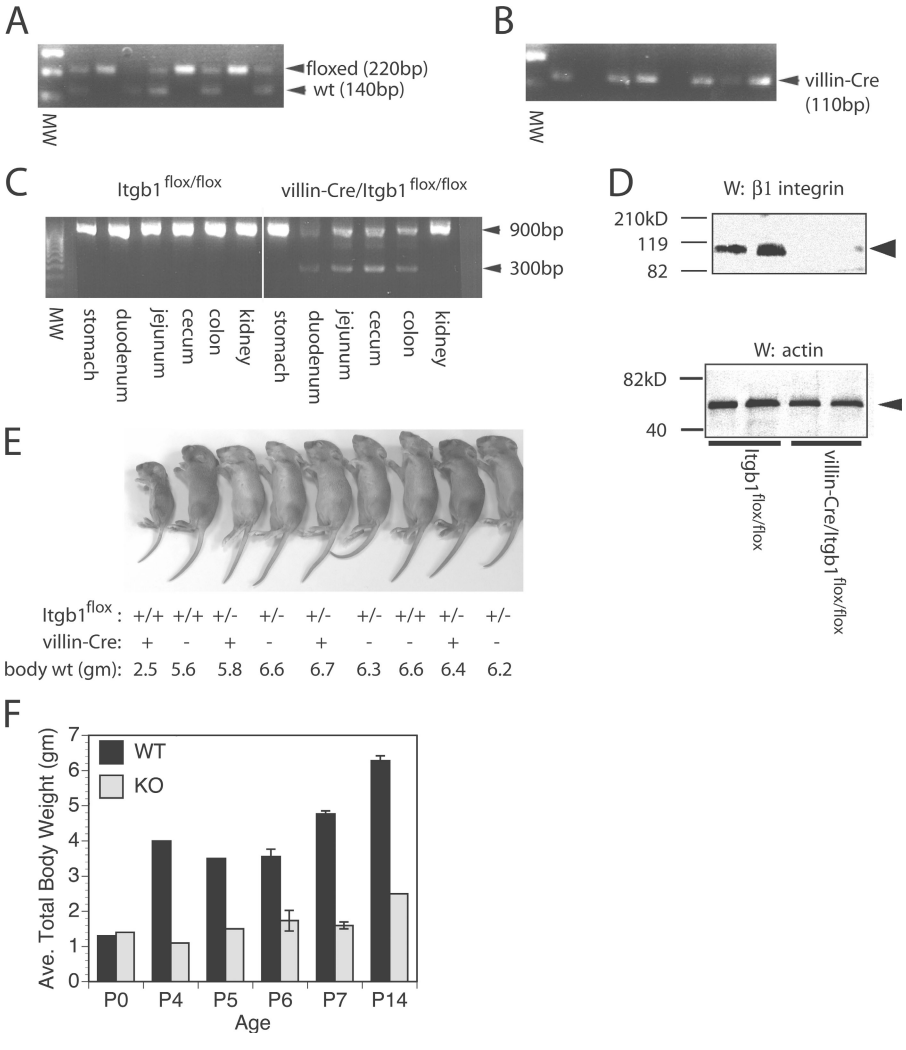

Figure 1. **Conditional deletion of *Itgb1* in mouse intestinal epithelium.** (A and B) Agarose gels of PCR products of genomic DNA extracted from tail snips of mice hetero- or homozygous for *Itgb1*^{flox} (A) or expressing the *villin-Cre* transgene (B). (C) Agarose gel of PCR products of genomic DNA from whole intestine from *Itgb1*$^{flox/flox}$ (left) or *villin-Cre/Itgb1*$^{flox/flox}$ (right) mice. The 300-bp product indicates recombination of the floxed Itgb1 allele. (D) Western blot of β1 integrin generated from lysates of small intestinal epithelial homogenates from *Itgb1*$^{flox/flox}$ or *villin-Cre/Itgb1*$^{flox/flox}$ mice. Actin loading controls are shown. Each lane represents 100 μg of total protein. (E) A P14 *villin-Cre/Itgb1*$^{flox/flox}$ mouse (extreme left) was less than half the body weight of its control littermates. (F) Graph shows the mean total body weights (± SEM) of four litters of mice according to genotype (WT, *Itgb1*$^{flox/flox}$ or *villin-Cre/Itgb1*$^{flox/+}$; KO, *villin-Cre/Itgb1*$^{flox/flox}$).

apoptosis was similar (<2% of total IECs counted) in both types of mice (Fig. 2, A and B). There was no evidence of mucosal defects or inflammation (specifically, crypt abscesses, intraepithelial leukocytes, and loss of crypts) that would have arisen from barrier defects in the intestines of the *villin-Cre/Itgb1*$^{flox/flox}$ mice (Fig. 2, A and B). Conditional deletion of *Itgb1* in skin disrupted basement membrane formation (Brakebusch et al., 2000; Raghavan et al., 2000), but ultrastructural examination revealed no differences in basement membrane structure between the *villin-Cre/Itgb1*$^{flox/flox}$ mice and their control littermates (Fig. 2, C–F). These results suggest that other adhesion molecules mediate epithelial adhesion, survival, and basement membrane formation in the intestine.

The distal small and proximal large intestines of the *villin-Cre/Itgb1*$^{flox/flox}$ mice were noticeably larger in external diameter compared with their control littermates (Fig. 2, G and H). This was found to be due in part to a dramatic expansion of the intestinal stroma (Fig. S1, C and D), muscularis (Fig. S1, E and F), and ECM (Fig. S1, G–N).

The epithelium in the *villin-Cre/Itgb1*$^{flox/flox}$ mice was markedly expanded compared with the control littermates as well (Fig. 3). The intestinal crypts and villi of P14 *villin-Cre/Itgb1*$^{flox/flox}$ mice (Fig. 3, B, D, and F) were much larger than those of their control littermates (Fig. 3, A, C, and E). In addition, the majority of the crypts in the P14 *villin-Cre/Itgb1*$^{flox/flox}$ mice were dysplastic, as indicated by pseudostratified, enlarged and crowded nuclei, and abnormal crypt architecture in both the small (Fig. 3, B and D) and large intestines (Fig. 3 F). The crypt expansion, enlargement, and dysplasia were much more pronounced in the cecum, a specialized portion of the large intestine (Fig. 3 F). Villous enlargement with expansion of the stroma was apparent, and there were multiple polypoid structures in the small intestinal mucosa of the *villin-Cre/Itgb1*$^{flox/flox}$ mice (Fig. 4, B–D) but not in their control littermates (Fig. 4 A). The mucosa overlying the polyps was not dysplastic, indicating normal maturation of the villous epithelium. The polyps had the appearance of juvenile type polyps because of the stromal expansion and cystic dilation of the crypts (Desai et al., 1995; Fig. 4, C and D).

Formed stool was found in the large intestines of the *villin-Cre/Itgb1*$^{flox/flox}$ mice but was absent in the large intestines of their control littermates, suggesting diarrhea (Wang et al., 2002). The intestinal contents of the *villin-Cre/Itgb1*$^{flox/flox}$ mice stained positively for large fat droplets (unpublished data), which was not observed in the control littermates and indicated the presence of steatorrhea and fat malabsorption in the former mice. Fat is absorbed by enterocytes along the length of the small intestine, and examination of intestinal epithelium from *villin-Cre/Itgb1*$^{flox/flox}$ mice revealed large lipid inclusions within the villous enterocytes that were not present in their control littermates (Fig. 4, E and F). Total serum lipid levels were significantly reduced in the *villin-Cre/Itgb1*$^{flox/flox}$ mice compared with their control littermates (unpublished data), confirming the presence of fat malabsorption.

Because the *villin-Cre/Itgb1*$^{flox/flox}$ mice appeared to die from severe malnutrition between P7 and P14, the absorptive lineage of IECs (enterocytic) was examined. Expression of the enterocytic marker sodium hydrogen exchanger 3 (NHE3) was detected in the vast majority of the IECs of the villi of the *villin-Cre/Itgb1*$^{flox/flox}$ mice and their control littermates (Fig. 4, G and H), demonstrating the abundance of enterocytes in both mice. However, ultrastructural examination of the small intestinal epithelium of *villin-Cre/Itgb1*$^{flox/flox}$ mice by electron microscopy revealed a severely defective microvillus brush border on the apical surfaces of the villous enterocytes (Fig. 4, I and J). Microvilli greatly increase the surface area of the intestine for

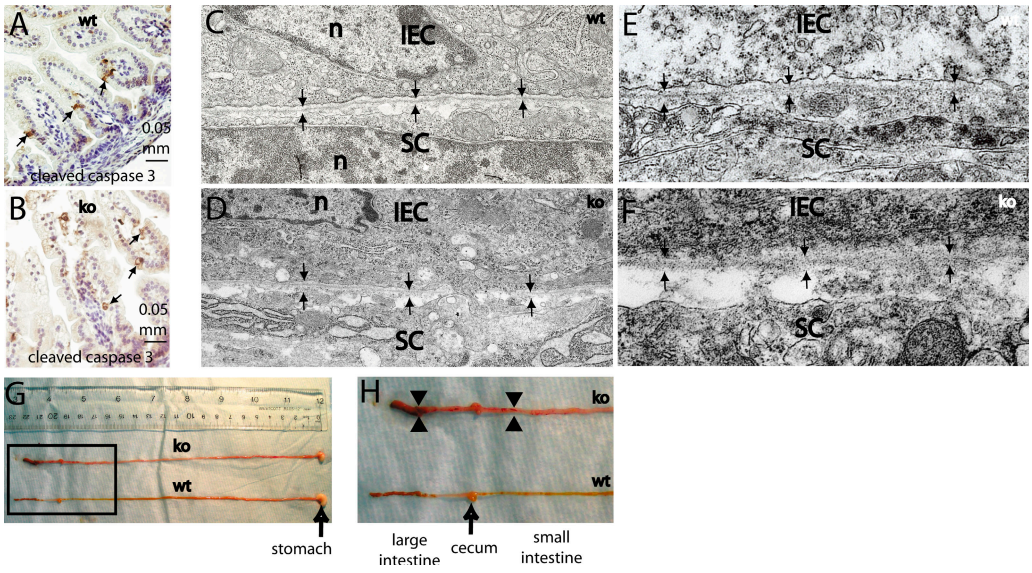

Figure 2. **Lack of increased intestinal apoptosis or basement membrane disruption in *villin-Cre/Itgb1*$^{flox/flox}$ mice.** (A and B) Immunohistochemical detection of cleaved caspase 3 (brown; arrows) positive IECs in small intestine of control (wt) and *villin-Cre/Itgb1*$^{flox/flox}$ mice (ko). Bars, 0.05 mm. (C–F) Transmission electron micrographs showing the basement membranes (arrows) in the ileum of control and *villin-Cre/Itgb1*$^{flox/flox}$ mice. SC, stromal cell; n, nucleus. (G) Gastrointestinal tracts resected from *villin-Cre/Itgb1*$^{flox/flox}$ (top) and *Itgb1*$^{flox/flox}$ (bottom) mice from Fig. 1 E. (H) The inset shows the larger diameters of the distal small intestine and proximal large intestine (black arrowheads) of the *villin-Cre/Itgb1*$^{flox/flox}$ mouse.

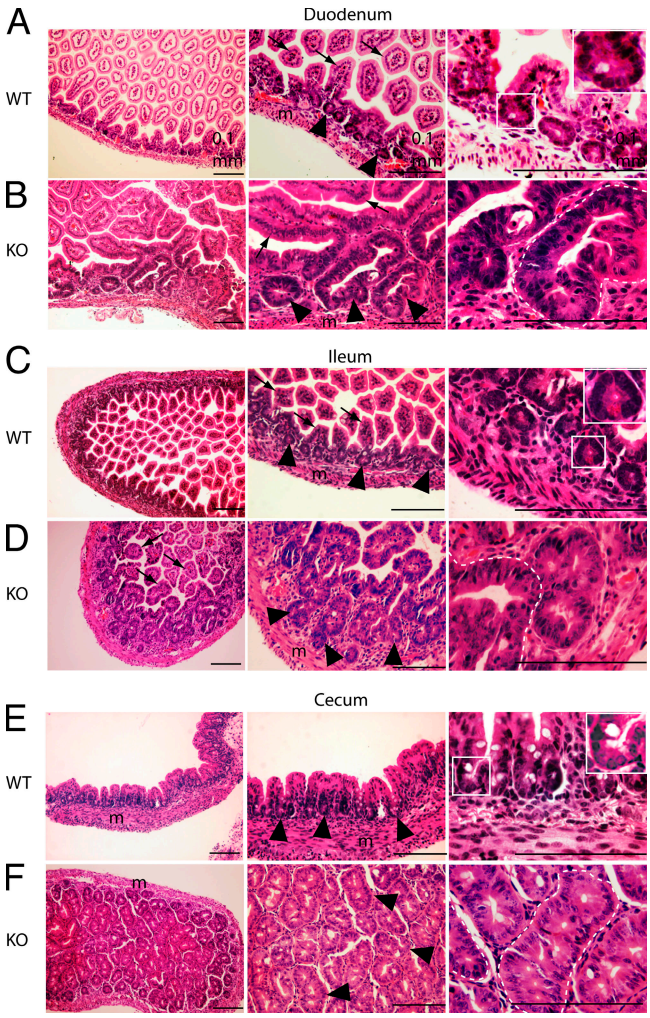

Figure 3. **Crypt hyperplasia and dysplasia and villous enlargement in *villin-Cre/Itgb1*$^{flox/flox}$ mice.** Hematoxylin-eosin sections of the intestines of P14 control (WT) and *villin-Cre/Itgb1*$^{flox/flox}$ (KO) littermates. Duodenal (A and B) and ileal (C and D) sections show markedly enlarged crypts (arrowheads) and villi (arrows) in the *villin-Cre/Itgb1*$^{flox/flox}$ mice (B and D) compared with those of the control littermate (A and C). m, muscularis layers. Normal crypts in the control mice are shown in the insets (A, C, and E). Dysplastic crypts in the *villin-Cre/Itgb1*$^{flox/flox}$ mice are outlined by dashed lines (B, D, and F). Sections through the cecum (large intestine) from a *villin-Cre/Itgb1*$^{flox/flox}$ mouse shows marked crypt hyperplasia (arrowheads in F) and dysplasia (dashed line) compared with a control littermate (E). Bars, 0.1 mm.

nutrient absorption, are essential for proper nutrition, and express nutrient transporters and digestive enzymes (Davidson et al., 1978). The intestinal microvilli were diminished in size and poorly formed in the *villin-Cre/Itgb1*$^{flox/flox}$ mice compared with their control littermates (Fig. 4, I and J), indicating defective enterocyte differentiation (Smith et al., 1986). Other IEC lineages were examined as well. The Paneth cell marker, Defensin/Cryptdin5, which was properly restricted to Paneth cells in control mice, was markedly increased in expression by the IECs along the entire crypt–villous axis of the *villin-Cre/Itgb1*$^{flox/flox}$ mice (Fig. S2, A and B, available at http://www.jcb.org/cgi/content/full/jcb.200602160/DC1). However, electron microscopy revealed that the villous IECs of the *villin-Cre/Itgb1*$^{flox/flox}$ mice expressed microvilli and lacked the secretory granules characteristic of true Paneth cells (unpublished data). The secretory goblet cell lineage was preserved in the *villin-Cre/Itgb1*$^{flox/flox}$ mice and their control littermates (Fig. S2, C and D) as well. Thus, proper cell fate determination occurred in the absence of β1 integrin expression.

The enlarged and dysplastic crypts in the *villin-Cre/Itgb1*$^{flox/flox}$ mice suggested that the aberrant epithelial proliferation could be responsible for the defective enterocytic differentiation. In the control mice, IECs with nuclear immunostaining for the cell cycle progression marker Ki-67 were confined to the crypt bases (Fig. 5 A) as expected. However, the number of IECs with nuclear Ki-67 was greatly increased in the crypts of the *villin-Cre/Itgb1*$^{flox/flox}$ mice (Fig. 5 B) compared with their control littermates. The *villin-Cre/Itgb1*$^{flox/flox}$ mice also demonstrated ectopic foci of Ki-67–positive IEC nuclei in the villi (Fig. 5, C and D), which were absent in the control littermates (Fig. 5 A). Immunodetection of Musashi-1, a putative intestinal stem cell marker (Potten et al., 2003) revealed an expansion of intestinal stem cells in the crypts of the *villin-Cre/Itgb1*$^{flox/flox}$ mice compared with their control littermates (Fig. 5, E and F). Musashi-1 was not detected in the villi of the *villin-Cre/Itgb1*$^{flox/flox}$ mice, suggesting that the ectopic foci of proliferating IECs were not stem cells mislocalized to the villi and were instead properly retained in the bottoms of the crypts. Thus, β1 integrin expression is not necessary for proper intestinal epithelial stem cell localization to the crypt bases.

During the first two postnatal weeks, crypt development in the mouse intestine occurs. Through the use of chimeric mice, it was previously shown that the nascent crypts are initially polyclonal and become monoclonal by P14, suggesting that stem cell selection occurs and yields a single pluripotent progenitor cell in each mature crypt (Wong et al., 2002). Genetic deletion of Tcf-4 in mice resulted in early postnatal lethality because of a complete lack of IEC proliferation in the nascent crypts, which led to intestinal failure shortly after birth (Korinek et al., 1998), demonstrating the essential role of Tcf-4 in intestinal stem cell proliferation and maintenance. Although the expression of nuclear Tcf-4 was limited to a few IECs in the bases of the nascent crypts in P6 control mice (Fig. 5 G), it was expressed by many more IECs in the nascent crypts and even the villi of P6 *villin-Cre/Itgb1*$^{flox/flox}$ mice (Fig. 5 H). Immunoblotting of nuclear lysates of the IECs confirmed the greater nuclear Tcf-4 protein expression in IECs of the *villin-Cre/Itgb1*$^{flox/flox}$ mice compared with IECs of their control littermates (Fig. 5 I). In addition, quantitative RT-PCR showed a significantly greater expression of Tcf-4 mRNA in the IECs from the *villin-Cre/Itgb1*$^{flox/flox}$ mice compared with IECs from their control littermates (Table I). Thus, β1 integrin deletion in the intestinal epithelium causes increased and mislocalized expression of Tcf-4 along the crypt–villous axis.

β1 integrins are well known to mediate cell proliferation through extracellular signal–regulated kinase (ERK) activation (for review see Giancotti, 1997). Examination of intestinal epithelial lysates from P6 *villin-Cre/Itgb1*$^{flox/flox}$ mice and their control littermates failed to show differences in ERK activation that could explain the large differences in IEC proliferation (Fig. 5 J). This result suggested that other proliferative signaling

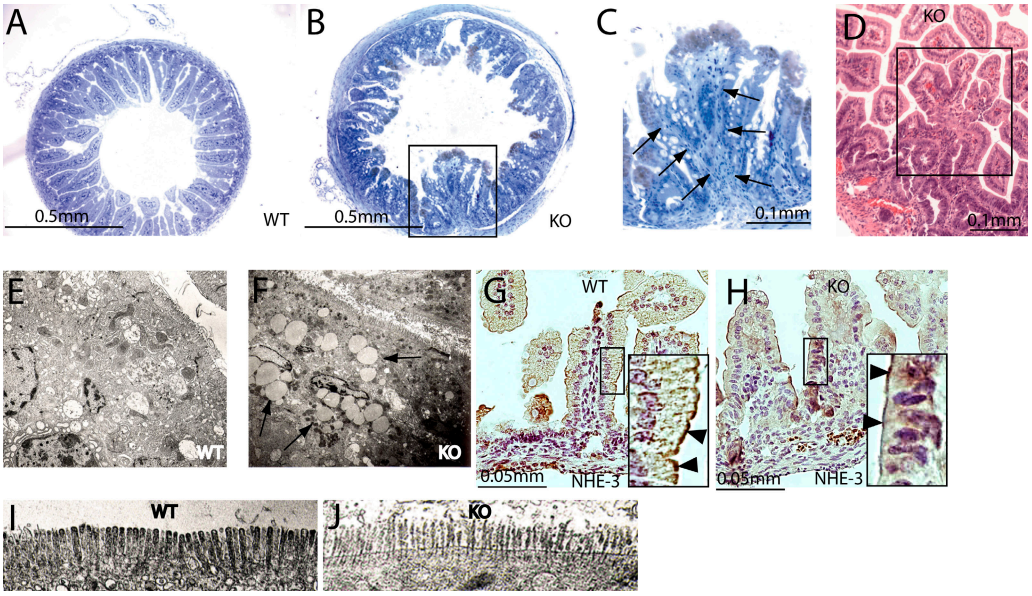

Figure 4. **Small intestinal polyps, lipid inclusions, and defective microvilli in *villin-Cre/Itgb1$^{flox/flox}$* mice.** (A–D) Transverse jejunal sections from P6 control (A) and *villin-Cre/Itgb1$^{flox/flox}$* (B–D) littermates show polyps with stromal expansion (arrows) in *villin-Cre/Itgb1$^{flox/flox}$* mice (C and D). The tissues were stained with glutaraldehyde and osmium tetroxide (A–C) or hematoxylin-eosin (D). (E and F) Transmission electron photomicrographs of jejunal enterocytes show lipid inclusions (arrows) in a P6 *villin-Cre/Itgb1$^{flox/flox}$* mouse (F) but not in the control littermate (E). (G and H) Immunohistochemical detection (brown) of the apical membrane/brush border enterocytic marker NHE3 (arrowheads) in jejunal sections from P6 control (G) and *villin-Cre/Itgb1$^{flox/flox}$* (H) mice. Insets show apical expression of NHE3. The insets show the apical membrane staining. (I and J) Transmission electron photomicrographs of microvilli on the apical cell membranes of jejunal enterocytes show abnormal morphology and sizes of microvilli in a P6 *villin-Cre/Itgb1$^{flox/flox}$* mouse (J) compared with a control littermate (I). Bars: (A and B) 0.5 mm; (C and D) 0.1 mm; (G and H) 0.05 mm.

pathways mediated the hyperproliferation observed in the intestinal epithelium of the *villin-Cre/Itgb1$^{flox/flox}$* mice.

The phenotypic changes observed in the *villin-Cre/Itgb1$^{flox/flox}$* mice (crypt hyperplasia, defective enterocyte differentiation, severe malnutrition, lipid inclusions, juvenile-like polyps, ectopic intestinal epithelial proliferation, and stromal expansion) were similar to those described in mice with defective Hedgehog signaling (Ramalho-Santos et al., 2000; Wang

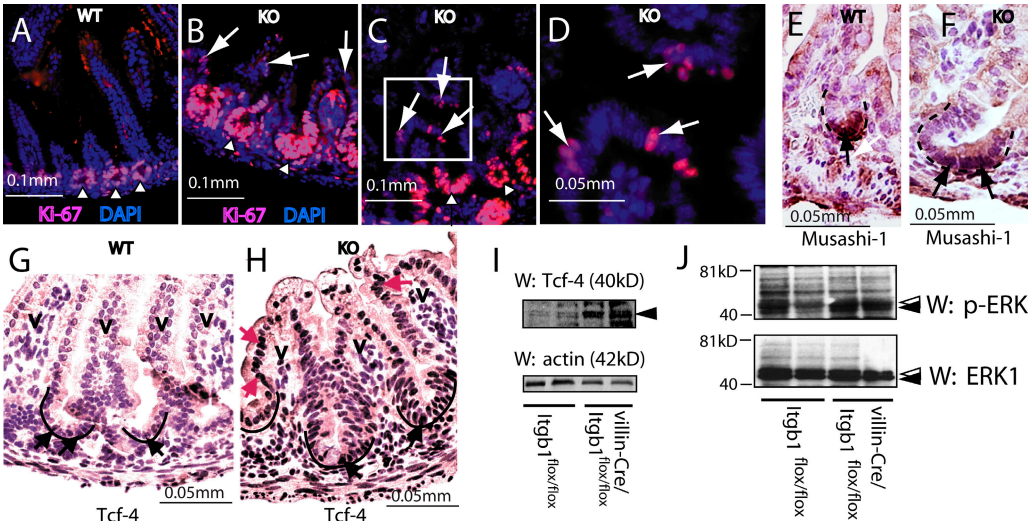

Figure 5. **Intestinal hyperproliferation in the *villin-Cre/Itgb1$^{flox/flox}$* mice.** (A–D) Ki-67 immunofluorescence (red; nuclei are shown in blue) reveals localization to IEC nuclei in the crypt bases (small arrows) in the jejunum of P6 control mice (A). Increased nuclear Ki-67 detection in the crypt (small arrows) and villous (large arrows) jejunal IECs of P6 *villin-Cre/Itgb1$^{flox/flox}$* mice (B and C). (D) Zoomed view of inset in C shows ectopic foci of Ki-67–positive nuclei in the villi. (E and F) Immunohistochemical detection of Musashi-1 in the jejunal crypts (outlined by black dashed lines) of P6 control (E) and *villin-Cre/Itgb1$^{flox/flox}$* (F) mice. (G and H) Immunohistochemical detection of Tcf-4 (brown) in nuclei of crypts (black arrows) and villous (red arrows) IECs in the jejunum of P6 control (G) and *villin-Cre/Itgb1$^{flox/flox}$* (H) mice. (I) Tcf-4 Western blot of nuclear lysates of jejunal IECs from P6 control and *villin-Cre/Itgb1$^{flox/flox}$* mice. All lanes contain 100 μg of total protein. (J) Phospho-ERK and ERK-1 Western blots performed on jejunal IEC lysates from P6 control and *villin-Cre/Itgb1$^{flox/flox}$* mice. The white and black arrowheads show p44 and p42 ERKs, respectively, in the top blot. The white arrowhead shows p-ERK, and the black arrowhead shows unphosphorylated ERK in the bottom blot. Bars: (A–C) 0.1 mm; (D–H) 0.05 mm.

Table I. **Quantitative RT-PCR results**

Gene	Control versus knockout
Tcf4	2.4 ± 0.4[a]
Ihh	−1.7 ± 0.1[a]
Shh	−60.5 ± 3.8[a]
Foxa2	−7.8 ± 2.0[a]

Results are expressed as the mean fold difference (± SEM) in mRNA levels between six pairs of P6 controls and their *villin-Cre/Itgb1*$^{flox/flox}$ littermates. A negative number reflects a decrease and a positive value an increase in the levels of PCR product in the knockout mouse samples compared with their control littermate samples. The RNA samples were extracted from the jejunum and normalized for total RNA concentration.
[a]$P < 0.05$.

et al., 2002; Madison et al., 2005). Thus, Hedgehog expression was examined.

Immunodetection and quantitative RT-PCR demonstrated large reductions of Shh and Ihh in the IECs of P6 *villin-Cre/Itgb1*$^{flox/flox}$ mice compared with their control littermates (Fig. 6 and Table I). In a previous study, neonatal mice with defective intestinal Hh signaling displayed the most severe changes in the distal ileum and cecum, the latter of which was enlarged (Wang et al., 2002). The crypt hyperplasia in the *villin-Cre/Itgb1*$^{flox/flox}$ mice was most dramatic in the distal small intestine, proximal large intestine, and cecum, which were enlarged in diameter as well (Fig. 2, G and H).

To determine if defective Hh signaling in the intestine could be a cause of aberrant expression of Tcf-4, neonatal mice were randomized to vehicle or the Hh inhibitor cyclopamine treatment for 7 d. Treatment with cyclopamine resulted in increased and mislocalized expression of Tcf-4 along the entire crypt–villous axis, suggesting that the dysregulation of Tcf-4 expression in the *villin-Cre/Itgb1*$^{flox/flox}$ mice may be due to diminished Hh expression and signaling (Fig. S2, E and F).

To further investigate the regulation of Hh expression by β1 integrins, studies on IECs were performed in vitro. Caco-2 cells differentiate into enterocyte-like and electrically resistant monolayers when postconfluent (Damstrup et al., 1999). As Caco-2 cells differentiated in culture, β1 integrin as well as Shh and Ihh expression increased (Fig. 7 A). Overexpression of β1 integrin in subconfluent Caco-2 cells in the presence of fibronectin caused increases in Ihh and Shh protein expression above constitutive levels (Fig. 7 B). β1 integrin overexpression in a rat intestinal epithelial (RIE) cell line with relatively low levels of Shh expression also increased Shh expression (Fig. 7 C). These results show that intestinal epithelial Hh expression requires an intact β1 integrin signaling pathway.

Because regional *Shh* expression in the central nervous system is dependent on HNF-3β (*Foxa2*; Epstein et al., 1999) and the *Shh* promoter contains consensus binding sites for HNF-3β (Chang et al., 1997; Kitazawa et al., 1998; Epstein et al., 1999; Odom et al., 2004), the role of HNF-3β in mediating β1 integrin–induced Shh expression was examined. HNF-3β protein levels were greatly decreased in nuclear lysates of IECs from P6 *villin-Cre/Itgb1*$^{flox/flox}$ mice compared with their control littermates (Fig. 7 D). Furthermore, HNF-3β mRNA levels were reduced approximately eightfold in *villin- Cre/Itgb1*$^{flox/flox}$

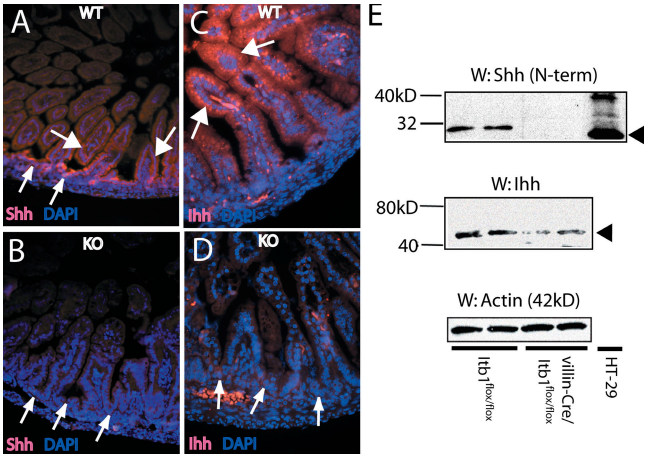

Figure 6. **Loss of Hedgehog expression in *villin-Cre/Itgb1*$^{flox/flox}$ mice.** (A and B) Immunofluorescent detection of Shh (red) shows crypt (small arrows) and villous (large arrows) small intestine epithelial expression in control (*Itgb1*$^{flox/flox}$) mice (A) but not in the *villin-Cre/Itgb1*$^{flox/flox}$ mice (B). The sections were stained with DAPI to demonstrate nuclei (blue). (C and D) Immunofluorescent detection of Indian hedgehog (Ihh) in the jejunal villi (large arrows) of a P6 control mouse (C) and *villin-Cre/Itgb1*$^{flox/flox}$ littermate (D). (E) Western blots of jejunal epithelial cell lysates show Shh, Ihh, and actin (loading controls) expression in two P6 *villin-Cre/Itgb1*$^{flox/flox}$ mice and their control littermates.

mice compared with their control littermates (Table I). These results suggest a dependence of HNF-3β expression on β1 integrin expression and signaling. Transfection of subconfluent Caco-2 cells (Fig. 7 E) with full-length human *FOXA2* induced SHH expression.

Because β1 integrins can modulate cell proliferation through activation of MAPK and PI3-kinase signaling, confluent RIE cells, which express relatively low constitutive levels of HNF-3β, were cultured in the presence of fibronectin and in the presence or absence of inhibitors of MEK-1 (PD98059) and PI3-kinase (LY294002) to determine how β1 integrins might regulate HNF-3β expression. Although MEK-1 inhibition failed to change HNF-3β expression (unpublished data), PI3-kinase inhibition caused HNF-3β expression to decrease (Fig. 7 F). When RIE cells with low levels of β1 integrin expression were transiently transfected with a full-length human β1 integrin construct, HNF-3β expression increased (Fig. 7 F). Furthermore, the PI3-kinase inhibitor LY294002 abrogated this β1 integrin–induced increase in HNF-3β expression (Fig. 7 F). These studies show that β1 integrin–PI3-kinase signaling stimulates HNF-3β expression, which in turn increases *Shh* transcription in IECs.

Discussion

Here, we show through the use of a genetic mouse model the key role of β1 integrins and, by inference, their ECM protein ligands in the regulation of IEC proliferation. The rapid turnover of enterocytes requires an early commitment to enterocytic cell fate and rapid differentiation of crypt IECs to achieve the vital function of nutrient absorption before the enterocytes are shed. As the IECs migrate out of the crypts and onto the villi, they undergo cell cycle arrest and differentiation (Gordon, 1989).

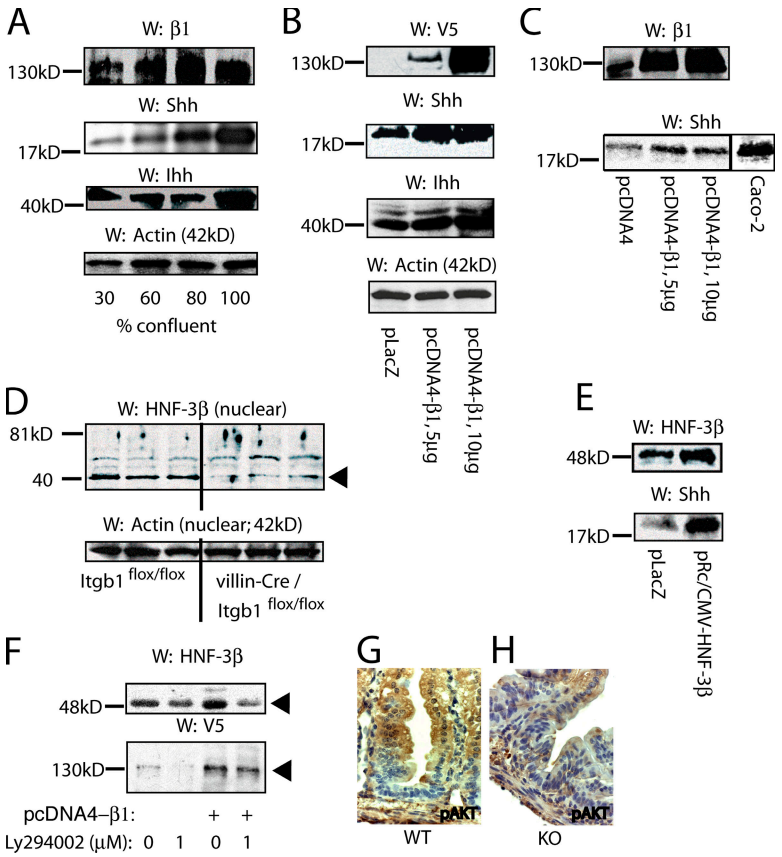

Figure 7. **β1 integrins regulate Hedgehog and HNF-3β (*Foxa2*) expression.** (A) Western blots of β1 integrin, Ihh, and Shh from cell lysates from Caco-2 cells that were allowed to differentiate in culture. (B) Western blots of V5 (C-terminal epitope-tagged human β1 integrin), Ihh, and Shh 48 h after transient transfection of Caco-2 cells with a full-length human *Itgb1* construct. (C) Western blots of β1 integrin and Shh from lysates of rat IECs transiently transfected with a vector alone or human β1 integrin construct (pcDNA4-β1). (D) Western blots of HNF-3β and actin generated from nuclear lysates of jejunal IECs from P6 *villin-Cre/Itgb1*$^{flox/flox}$ mice and their control littermates. (E) Western blots of HNF-3β and Shh generated from lysates of Caco-2 cells 48 h after transient transfection with a control vector (pLacZ) or plasmids containing a full-length human HNF-3β (*FOXA2*) construct. (F) Western blot of HNF-3β and V5 epitope of lysates of rat IECs transiently transfected with pcDNA4-β1-V5 or vector alone. After transfection, the cells were incubated with or without the PI3-kinase inhibitor LY294002.

The lack of regulation of intestinal epithelial proliferation in the *villin-Cre/Itgb1*$^{flox/flox}$ mouse likely contributed to defective enterocytic differentiation and fat malabsorption, which contributed to their postnatal lethality. However, we cannot conclude from our data that deletion of β1 integrins negatively affected IEC differentiation independent of IEC proliferation.

The epithelial crypt hyperproliferation and dysplasia in the *villin-Cre/Itgb1*$^{flox/flox}$ mice were unexpected because β1 integrins were previously shown to promote anchorage-dependent cell proliferation in a variety of cells and tissues (for review see Lee and Juliano, 2004) and growth factor–induced nuclear translocation of activated ERK (Zhu and Assoian, 1995; Wary et al., 1996, 1998; Aplin et al., 2001). Conditional deletion of β1 integrins in the epidermal and mammary epithelia, but not in intestinal epithelium, caused decreased epithelial stem cell proliferation and ERK activation (Brakebusch et al., 2000; Raghavan et al., 2000; Faraldo et al., 2001). A major difference between β1 integrin deletion in the intestinal epithelium compared with epidermal or mammary epithelium was that the structure of the basement membrane and epithelial cell adhesion were disrupted in the epidermal and mammary epithelia (Brakebusch et al., 2000; Raghavan et al., 2000; Faraldo et al., 2001) but maintained in the intestinal epithelium.

That conditional deletion of β1 integrins in the intestinal epithelium of mice failed to cause defects in IEC adhesion or survival was somewhat surprising because inhibition of β1 integrin–mediated adhesion in IECs ex vivo resulted in anoikis (Strater et al., 1996; Lee and Juliano, 2000). A large disruption of IEC adhesion during the neonatal period, a time when the intestine becomes rapidly colonized with bacteria, would have resulted in necrotizing enterocolitis because of a loss of the mucosal barrier (Hackam et al., 2005), which was not observed. Thus, the maintenance of anchorage of the IECs to a normal basement membrane in the *villin-Cre/Itgb1*$^{flox/flox}$ mice suggests that the principal function of β1 integrins in the intestinal epithelium during intestinal development is not cell anchorage but ECM-induced regulation of epithelial proliferation.

The phenotypic changes of the *villin-Cre/Itgb1*$^{flox/flox}$ mice and neonatal mice with defective Hh expression or signaling (Ramalho-Santos et al., 2000; Wang et al., 2002; Madison et al., 2005) are strikingly similar. Although the expression of the Hh receptor Patched and downstream signaling proteins Smoothened and Gli were unaffected (unpublished data), the expression of Shh and Ihh was greatly reduced in the *villin-Cre/Itgb1*$^{flox/flox}$ mice. Furthermore, transient expression of β1 integrin in IECs increased Shh expression. These novel results demonstrate that Hh expression is dependent on β1 integrin expression and signaling in the intestinal epithelium.

Although the intensity of Hh signaling is regulated through several important posttranslational steps (Porter et al., 1995, 1996; Pepinsky et al., 2002), what governs transcriptional regulation and expression of Hhs is poorly understood. The expression of the Forkhead family transcription factor HNF-3β (Foxa2), which is involved in Shh expression (Chang et al., 1997; Kitazawa et al., 1998; Epstein et al., 1999; Odom et al., 2004), was significantly reduced in the *villin-Cre/Itgb1*$^{flox/flox}$

mice, and overexpression of HNF-3β in IECs stimulated Shh expression. Thus, β1 integrins may mediate Shh expression via HNF-3β in IECs.

Which α/β1 integrin heterodimers contribute to Hh expression in the intestinal tissues is presently unknown. Fibronectin is expressed in the intestinal crypts and α5/β1 integrin, the classical fibronectin receptor, along the crypt–villous axis (Beaulieu et al., 1991; Beaulieu, 1992). Although fibronectin expression was increased in the stroma of the *villin-Cre/Itgb1*$^{flox/flox}$ mice, α5/β1 integrin expression was lost in comparison with their control littermates (Fig. S2, G and H). Expression of α5/β1 integrin in Caco-2 and HT-29 intestinal cells, which lack α5/β1 integrin expression, increased Shh protein expression in the presence of fibronectin (Fig. S2 I). These studies suggest that α5/β1 integrin expression may be important for Shh expression in the intestinal epithelium.

The intestinal crypt hyperplasia and dysplasia in the *villin-Cre/Itgb1*$^{flox/flox}$ mice were similar to findings in mice in which *Apc* was conditionally deleted in the intestinal epithelium (Andreu et al., 2005). Epithelial dysplasia is the earliest neoplastic change preceding macroscopic adenomatous polyp formation in the intestine and is most commonly associated with *APC* mutations in human and mouse intestines (Levy et al., 1994; Luongo et al., 1994). Crypt dysplasia occurred within 3–4 d after induction of *Apc* deletion in the intestinal epithelium but, similar to the *villin-Cre/Itgb1*$^{flox/flox}$ mice, the overlying villous epithelium was not dysplastic (Andreu et al., 2005). The unexpected finding of crypt dysplasia after the conditional deletion of intestinal epithelial β1 integrins may relate to the previous observations that β1 integrins are decreased in expression during human intestinal carcinogenesis and can abrogate tumorigenesis when expressed in colon cancer cells (Stallmach et al., 1992, 1994; Varner et al., 1995; Kuwada et al., 2005). It is presently unknown if the dysplastic crypts would have given rise to adenomas in the *villin-Cre/Itgb1*$^{flox/flox}$ or *Apc*-deleted mice because they all died rapidly after birth and APC deletion, respectively.

The increased expression of the putative intestinal stem cell marker Musashi-1 in the crypt IECs of the *villin-Cre/Itgb1*$^{flox/flox}$ mice compared with their control littermates suggests that β1 integrins are important in regulating intestinal stem cell proliferation and prompted examination of Tcf-4 expression in the *villin-Cre/Itgb1*$^{flox/flox}$ mice. Tcf-4 expression is normally restricted to IECs in the crypt bases in neonatal mice (Barker et al., 1999); however, its expression was increased and mislocalized along the entire crypt–villous axis of the *villin-Cre/Itgb1*$^{flox/flox}$ mice. Inhibition of Hh signaling increased Wnt gene expression in the mouse intestinal epithelium (Madison et al., 2005), and Ihh was shown to inhibit Tcf-4 expression in colon cancer cells (van den Brink et al., 2004). Furthermore, Tcf-4 protein expression was increased and mislocalized along the entire crypt–villous axis in neonatal mice treated with the Hh signaling inhibitor cyclopamine (Fig. S2, E and F). These findings suggest that Hh signaling regulates Tcf-4 expression in the intestinal epithelium.

β-Catenin protein expression levels and nuclear localization were similar between the IECs of the *villin-Cre/Itgb1*$^{flox/flox}$ mice and their control littermates by Western blot and immunofluorescence (Fig. S2, J–L), suggesting that canonical Wnt signaling was not increased in the former mice. Recently, it was shown that Tcf-4 can mediate proliferative and noncanonical Wnt signaling (Nateri et al., 2005). Thus, it is possible that the increased Tcf-4 expression in the intestinal epithelium of *villin-Cre/Itgb1*$^{flox/flox}$ mice may heighten the sensitivity of IECs to key proliferative signaling pathways.

In summary, this study shows that β1 integrins regulate Hh expression in the intestinal epithelium and are required for the proper compartmentalization and regulation of intestinal proliferation. Because the Hh receptor Patched has been shown to be localized to stromal cells in the intestine (Ramalho-Santos et al., 2000; Madison et al., 2005), it is likely that the ability of Hhs to regulate intestinal proliferation is stromal dependent. Finally, the dispensability of β1 integrins for intestinal basement membrane formation and epithelial anchorage, but requirement for intestinal epithelial and stromal regulation, exemplifies their strategic role as mediators of epithelial–stromal cross talk.

Materials and methods

Mice

The *villin-Cre* and *Itgb1*^{flox} mice were previously described (Brakebusch et al., 2000; Raghavan et al., 2000). *Villin-Cre* and *Itgb1*^{flox} mice were mated and the offspring were backcrossed to generate *villin-Cre/Itgb1*$^{flox/flox}$ mice. Genotyping was performed on genomic DNA isolated from tail snips or whole intestine as previously described (Brakebusch et al., 2000; Raghavan et al., 2000). The pups were killed when they displayed lethargy and inability to feed. The intestines and other organs were harvested, washed in PBS, and fixed in formalin overnight or frozen in an ethanol–dry ice bath. All animal studies were approved by the Institutional Animal Care and Use Committees at the University of Utah and Salt Lake City Veterans Affairs Health Care System. The *Itgb1*^{flox} mice were a gift from E. Fuchs (The Rockefeller University, New York, NY).

Antibodies

The following antibodies were used: HNF-3β, Ihh, Shh (N-terminal), and Tcf-4 pAb (Santa Cruz Biotechnology, Inc.) polyclonal antibodies; integrin α5 mAb (BD Biosciences); Ki-67 mAb (BD Biosciences); integrin β1 mAb and collagen I, collagen IV, fibronectin, and laminin polyclonal antibodies (Chemicon); and actin mAb (Neomarkers).

Immunohistochemistry

Fixed tissues were embedded in paraffin as described previously (Scaife et al., 2002). The samples were deparaffinized in xylene and rehydrated in a 30–100% ethanol series and ddH_2O. Antigen retrieval was performed by boiling the samples in 10 mM Citrate Buffer, pH 6.0, in a microwave oven. The slides were then washed with 1× PBS for 5 min at RT. The samples were blocked in 3% horse serum, 3% bovine calf serum, or 3% goat serum in 0.1% Triton X-100/1% BSA in PBS for 30 min at RT in a humidity chamber. Primary antibody dilutions in the blocking buffer were incubated with the samples overnight in a humidity chamber at RT.

The slides were washed in PBS and a secondary antibody conjugated to Alexa 488 (diluted in blocking buffer) was added to the samples for 30 min at RT. The slides were washed in PBS and then mounted with Prolong-Gold and coverslips. All pairs of slides were processed simultaneously, and all pairs of photomicrographs were performed with identical camera settings and exposure times to ensure uniformity.

For immunohistochemical detection, the samples were first deparaffinized and rehydrated as above. The endogenous peroxidases were quenched with 3% H_2O_2 in PBS or 1× TBS for 10 min at RT. The slides were then washed with 1× TBS or 1× PBS. Antigen retrieval (which must be optimized for each tissue) was performed by adding Target Retrieval Solution (DakoCytomation) for 30 min at 90°C. The slides were washed with PBS. The samples were blocked in 3% bovine calf serum, 3% goat serum, or 3% horse serum in 1% BSA in PBS depending on the species used to generate the primary antibody. All incubation steps were done in

a humidified chamber. At this point, we used the immuno or pap pen to mark an aqueous barrier around each tissue. Antibody incubation was performed as above except that a horseradish peroxidase–conjugated secondary antibody was used. The slides were incubated in ABC reagent (Vector Laboratories) for various times up to 30 min. The slides were washed in 1× TBS. The reaction was stopped by placing the slides in ddH_2O. The slides were counterstained with hematoxylin for 1 min. The slides were dehydrated in a 70–100% ethanol series and xylene. The slides were mounted with coverslips.

All images were obtained at RT with a microscope (AX70; Olympus), which is equipped with the following objectives: 4× (0.16 NA), 20× (0.7 NA), 40× (0.85 NA), 60× oil (1.4 NA), and 100× oil (0.5–1.35 NA). The images were digitally recorded via an AxioCam (Carl Zeiss MicroImaging, Inc.) and saved using the AxioVision program (Carl Zeiss MicroImaging, Inc.). The images were imported into Illustrator (Adobe). All images for each protein were collected using the same exposure times to ensure uniformity amongst the samples. Overlays of the immunofluorescence images were performed in Photoshop (Adobe). The scales of the images obtained with each specific objective are maintained in each respective figure in the manuscript to allow direct comparisons of the sizes of objects within each figure.

IEC isolation and nuclear lysate preparation

IECs from mouse intestines were isolated as previously described (Whitehead et al., 1987). Nuclear lysates were prepared from IECs using the following protocol: the IECs obtained above were washed in PBS and pelleted at 300 rpm at RT for 3 min. The PBS was removed, and the cells were resuspended in ice-cold 200 μl Buffer A (20 mM Hepes, pH 7.4), 1 mm EDTA, 1 mM EGTA, 10% glycerol, and 0.2% NP-40; just before use, a protease inhibitor cocktail (aprotinin, 10 μg/ml leupeptin, 10 μl Na_3VO_4 [0.2 mM], 50 μl Dithiothreitol [1 mM], and 50 μl PMSF [0.5 mM]) was added. The cells were vortexed five times for 10 s each. The lysates were centrifuged at 500 *g* for 5 min at 4°C, and the supernatants (cytoplasmic fraction) were removed. 50 μl of Buffer B (20 mM Hepes, pH 7.4), 1 mM EDTA, 1 mM EGTA, 10% glycerol, 0.2% NP-40, and protease inhibitor cocktail (see above) were added just before use. The cells were vortexed five times for 10 s each, and the lysates were incubated on ice for 30 min. The lysates were centrifuged at 13,000 *g* for 10 min at 4°C, and supernatants (nuclear preparations) were removed.

Immunoblotting

Whole intestine was homogenized in lysis buffer (50 mM Hepes, 150 mM NaCl, 1.5 mM $MgCl_2$, 1 mM EGTA, 100 mM NaF, 10 mM Na_2PO_4, 1 mM Na_3VO_4, 10% glycerol, 1% Triton X-100, and 1 μg/ml each of aprotinin, leupeptin, chymostatin, and pepstatin) on ice. The homogenates were then sonicated for 10 s and clarified by centrifuging at 14,000 *g* for 15 min at 4°C. The Triton soluble and insoluble pellets were boiled in sample buffer (125 mM Tris-HCl, pH 6.8, 20% glycerol, 4% sodium dodecyl sulfate, 2% β-mercaptoethanol, and 10 μg/ml bromophenol blue) for 3 min. Western blots were generated as previously described (Kuwada et al., 2005).

Quantitative RT-PCR

Total RNA was isolated in RNeasy kit (QIAGEN) from sections (~3 × 3 × 3 mm) of freshly resected intestine or purified IECs (Whitehead et al., 1987). First-strand cDNA was synthesized from 1 μg of total RNA using M-MLV reverse transcriptase (Invitrogen). Quantitative RT-PCR was performed using SybrGreen incorporation or Taqman primer probe sets on a Sequence Detection System (ABI PRISM 7900HT; Applied Biosystems). Threshold cycles for TaqMan primers were normalized to threshold cycles for actin, and threshold cycles for SybrGreen primers were normalized to glyceraldehyde-3-phosphate dehydrogenase (G3PDH).

TaqMan primer and probe sets were purchased from Applied Biosciences for Tcf-4, actin, and Shh. The following are primer sets designed for SybrGreen incorporation. The primers were designed to span intron–exon boundaries. For the mouse primer sets, the temperature was 80–84°C. Ihh, 5′ TTCAAGGACGAGGAGAACACG 3′ and 5′ TTCAGACG GTCCTTGCAGC 3′; G3PDH, 5′ CAGTGCTGAGTATGTCGTGG 3′ and 5′ AGAACGGACGGAGATGATGACC 3′.

Statistical analysis

Quantitative PCR results were compared by analyzing the differences in the midpoints of the linear phases of the appearance of double-stranded DNA products using Sybr Green for six pairs of knockout and control mice. Each gene expression product was normalized against G3PDH for that sample before the comparisons. A two-sided *t* test with unequal variance was used to statistically compare the results. The mean nonfasting cholesterol and triglyceride levels were determined (Anilytics) on serum levels and compared using a *t* test.

Transfection

Caco-2 and IEC-6 RIE cells (American Type Culture Collection) were cultured in DME supplemented with 10% fetal bovine serum, glutamine, penicillin, and streptomycin to ~70% confluency on plain or fibronectin-coated dishes. Transient transfections of a full-length human pcDNA4 (Invitrogen), pLacZ, *ITGB1* construct (pcDNA4-*ITGB1*), or pRc/CMV-*FOXA2* (a gift from V. Besnard, Cincinnati Children's Medical Center, Cincinnati, OH) were performed with Lipofectamine (Invitrogen) reagent as previously described (Kuwada et al., 2005). The full-length human *Itgb1* gene was digested from pECE-α5 (a gift from E. Ruoslahti, Burnham Institute, La Jolla, CA) with EcoRI and ligated into the EcoRI site of pcDNA4 (Invitrogen).

Online supplemental material

Fig. S1 shows ECM protein expression patterns in the intestines of control and conditional β1 integrin knockout mice. Fig. S2 shows intestinal epithelial lineage markers, α5/β1 integrin expression, and β-catenin expression in control and conditional β1 integrin knockout mice, as well as Tcf-4 expression in mice treated with the Hedgehog signaling inhibitor cyclopamine. Online supplemental material is available at http://www.jcb.org/cgi/content/full/jcb.200602160/DC1.

This work was supported by grants from the National Institutes of Health (DK02531), Huntsman Cancer Foundation, and Veterans Affairs Administration.

Submitted: 28 February 2006
Accepted: 6 October 2006

References

Abbi, S., H. Ueda, C. Zheng, L.A. Cooper, J. Zhao, R. Christopher, and J.L. Guan. 2002. Regulation of focal adhesion kinase by a novel protein inhibitor FIP200. *Mol. Biol. Cell.* 13:3178–3191.

Andreu, P., S. Colnot, C. Godard, S. Gad, P. Chafey, M. Niwa-Kawakita, P. Laurent-Puig, A. Kahn, S. Robine, C. Perret, and B. Romagnolo. 2005. Crypt-restricted proliferation and commitment to the Paneth cell lineage following Apc loss in the mouse intestine. *Development.* 132:1443–1451.

Aplin, A.E., S.A. Stewart, R.K. Assoian, and R.L. Juliano. 2001. Integrin-mediated adhesion regulates ERK nuclear translocation and phosphorylation of Elk-1. *J. Cell Biol.* 153:273–282.

Barker, N., G. Huls, V. Korinek, and H. Clevers. 1999. Restricted high level expression of Tcf-4 protein in intestinal and mammary gland epithelium. *Am. J. Pathol.* 154:29–35.

Beaulieu, J.F. 1992. Differential expression of the VLA family of integrins along the crypt-villus axis in the human small intestine. *J. Cell Sci.* 102:427–436.

Beaulieu, J.F., P.H. Vachon, and S. Chartrand. 1991. Immunolocalization of extracellular matrix components during organogenesis in the human small intestine. *Anat. Embryol. (Berl.).* 183:363–369.

Brakebusch, C., R. Grose, F. Quondamatteo, A. Ramirez, J.L. Jorcano, A. Pirro, M. Svensson, R. Herken, T. Sasaki, R. Timpl, et al. 2000. Skin and hair follicle integrity is crucially dependent on beta 1 integrin expression on keratinocytes. *EMBO J.* 19:3990–4003.

Chang, B.E., P. Blader, N. Fischer, P.W. Ingham, and U. Strahle. 1997. Axial (HNF3beta) and retinoic acid receptors are regulators of the zebrafish sonic hedgehog promoter. *EMBO J.* 16:3955–3964.

Clark, E.A., and J.S. Brugge. 1995. Integrins and signal transduction pathways: the road taken. *Science.* 268:233–239.

Damstrup, L., S.K. Kuwada, P.J. Dempsey, C.L. Brown, C.J. Hawkey, H.S. Poulsen, H.S. Wiley, and R.J. Coffey Jr. 1999. Amphiregulin acts as an autocrine growth factor in two human polarizing colon cancer lines that exhibit domain selective EGF receptor mitogenesis. *Br. J. Cancer.* 80:1012–1019.

Davidson, G.P., E. Cutz, J.R. Hamilton, and D.G. Gall. 1978. Familial enteropathy: a syndrome of protracted diarrhea from birth, failure to thrive, and hypoplastic villus atrophy. *Gastroenterology.* 75:783–790.

Dekaney, C.M., J.M. Rodriguez, M.C. Graul, and S.J. Henning. 2005. Isolation and characterization of a putative intestinal stem cell fraction from mouse jejunum. *Gastroenterology.* 129:1567–1580.

Desai, D.C., K.F. Neale, I.C. Talbot, S.V. Hodgson, and R.K. Phillips. 1995. Juvenile polyposis. *Br. J. Surg.* 82:14–17.

Epstein, D.J., A.P. McMahon, and A.L. Joyner. 1999. Regionalization of Sonic hedgehog transcription along the anteroposterior axis of the mouse central nervous system is regulated by Hnf3-dependent and -independent mechanisms. *Development.* 126:281–292.

Faraldo, M.M., M.A. Deugnier, J.P. Thiery, and M.A. Glukhova. 2001. Growth defects induced by perturbation of beta1-integrin function in the mammary gland epithelium result from a lack of MAPK activation via the Shc and Akt pathways. *EMBO Rep.* 2:431–437.

Fujimoto, K., R.D. Beauchamp, and R.H. Whitehead. 2002. Identification and isolation of candidate human colonic clonogenic cells based on cell surface integrin expression. *Gastroenterology.* 123:1941–1948.

Giancotti, F.G. 1997. Integrin signaling: specificity and control of cell survival and cell cycle progression. *Curr. Opin. Cell Biol.* 9:691–700.

Gordon, J.I. 1989. Intestinal epithelial differentiation: new insights from chimeric and transgenic mice. *J. Cell Biol.* 108:1187–1194.

Hackam, D.J., J.S. Upperman, A. Grishin, and H.R. Ford. 2005. Disordered enterocyte signaling and intestinal barrier dysfunction in the pathogenesis of necrotizing enterocolitis. *Semin. Pediatr. Surg.* 14:49–57.

Howe, J.R., S. Roth, J.C. Ringold, R.W. Summers, H.J. Jarvinen, P. Sistonen, I.P. Tomlinson, R.S. Houlston, S. Bevan, F.A. Mitros, et al. 1998. Mutations in the SMAD4/DPC4 gene in juvenile polyposis. *Science.* 280:1086–1088.

Howe, J.R., J.L. Bair, M.G. Sayed, M.E. Anderson, F.A. Mitros, G.M. Petersen, V.E. Velculescu, G. Traverso, and B. Vogelstein. 2001. Germline mutations of the gene encoding bone morphogenetic protein receptor 1A in juvenile polyposis. *Nat. Genet.* 28:184–187.

Kedinger, M., I. Duluc, C. Fritsch, O. Lorentz, M. Plateroti, and J.N. Freund. 1998. Intestinal epithelial-mesenchymal cell interactions. *Ann. N. Y. Acad. Sci.* 859:1–17.

Kitazawa, S., R. Kitazawa, H. Tamada, and S. Maeda. 1998. Promoter structure of human sonic hedgehog gene. *Biochim. Biophys. Acta.* 1443:358–363.

Korinek, V., N. Barker, P. Moerer, E. van Donselaar, G. Huls, P.J. Peters, and H. Clevers. 1998. Depletion of epithelial stem-cell compartments in the small intestine of mice lacking Tcf-4. *Nat. Genet.* 19:379–383.

Kuhnert, F., C.R. Davis, H.T. Wang, P. Chu, M. Lee, J. Yuan, R. Nusse, and C.J. Kuo. 2004. Essential requirement for Wnt signaling in proliferation of adult small intestine and colon revealed by adenoviral expression of Dickkopf-1. *Proc. Natl. Acad. Sci. USA.* 101:266–271.

Kuwada, S.K., J. Kuang, and X. Li. 2005. Integrin alpha5/beta1 expression mediates HER-2 down-regulation in colon cancer cells. *J. Biol. Chem.* 280:19027–19035.

Lee, J.W., and R.L. Juliano. 2000. alpha5beta1 integrin protects intestinal epithelial cells from apoptosis through a phosphatidylinositol 3-kinase and protein kinase B-dependent pathway. *Mol. Biol. Cell.* 11:1973–1987.

Lee, J.W., and R. Juliano. 2004. Mitogenic signal transduction by integrin- and growth factor receptor-mediated pathways. *Mol. Cells.* 17:188–202.

Levy, D.B., K.J. Smith, Y. Beazer-Barclay, S.R. Hamilton, B. Vogelstein, and K.W. Kinzler. 1994. Inactivation of both APC alleles in human and mouse tumors. *Cancer Res.* 54:5953–5958.

Luongo, C., A.R. Moser, S. Gledhill, and W.F. Dove. 1994. Loss of Apc+ in intestinal adenomas from Min mice. *Cancer Res.* 54:5947–5952.

Madison, B.B., L. Dunbar, X.T. Qiao, K. Braunstein, E. Braunstein, and D.L. Gumucio. 2002. Cis elements of the villin gene control expression in restricted domains of the vertical (crypt) and horizontal (duodenum, cecum) axes of the intestine. *J. Biol. Chem.* 277:33275–33283.

Madison, B.B., K. Braunstein, E. Kuizon, K. Portman, X.T. Qiao, and D.L. Gumucio. 2005. Epithelial hedgehog signals pattern the intestinal crypt-villus axis. *Development.* 132:279–289.

Nateri, A.S., B. Spencer-Dene, and A. Behrens. 2005. Interaction of phosphorylated c-Jun with TCF4 regulates intestinal cancer development. *Nature.* 437:281–285.

Odom, D.T., N. Zizlsperger, D.B. Gordon, G.W. Bell, N.J. Rinaldi, H.L. Murray, T.L. Volkert, J. Schreiber, P.A. Rolfe, D.K. Gifford, et al. 2004. Control of pancreas and liver gene expression by HNF transcription factors. *Science.* 303:1378–1381.

Pepinsky, R.B., R.I. Shapiro, S. Wang, A. Chakraborty, A. Gill, D.J. Lepage, D. Wen, P. Rayhorn, G.S. Horan, F.R. Taylor, et al. 2002. Long-acting forms of Sonic hedgehog with improved pharmacokinetic and pharmacodynamic properties are efficacious in a nerve injury model. *J. Pharm. Sci.* 91:371–387.

Pinto, D., A. Gregorieff, H. Begthel, and H. Clevers. 2003. Canonical Wnt signals are essential for homeostasis of the intestinal epithelium. *Genes Dev.* 17:1709–1713.

Porter, J.A., D.P. von Kessler, S.C. Ekker, K.E. Young, J.J. Lee, K. Moses, and P.A. Beachy. 1995. The product of hedgehog autoproteolytic cleavage active in local and long-range signalling. *Nature.* 374:363–366.

Porter, J.A., K.E. Young, and P.A. Beachy. 1996. Cholesterol modification of hedgehog signaling proteins in animal development. *Science.* 274:255–259.

Potten, C.S., and M. Loeffler. 1990. Stem cells: attributes, cycles, spirals, pitfalls and uncertainties. Lessons for and from the crypt. *Development.* 110:1001–1020.

Potten, C.S., C. Booth, G.L. Tudor, D. Booth, G. Brady, P. Hurley, G. Ashton, R. Clarke, S. Sakakibara, and H. Okano. 2003. Identification of a putative intestinal stem cell and early lineage marker; musashi-1. *Differentiation.* 71:28–41.

Raghavan, S., C. Bauer, G. Mundschau, Q. Li, and E. Fuchs. 2000. Conditional ablation of beta1 integrin in skin. Severe defects in epidermal proliferation, basement membrane formation, and hair follicle invagination. *J. Cell Biol.* 150:1149–1160.

Ramalho-Santos, M., D.A. Melton, and A.P. McMahon. 2000. Hedgehog signals regulate multiple aspects of gastrointestinal development. *Development.* 127:2763–2772.

Scaife, C.L., J. Kuang, J.C. Wills, D.B. Trowbridge, P. Gray, B.M. Manning, E.J. Eichwald, R.A. Daynes, and S.K. Kuwada. 2002. Nuclear factor kappaB inhibitors induce adhesion-dependent colon cancer apoptosis: implications for metastasis. *Cancer Res.* 62:6870–6878.

Schwartz, M.A., and V. Baron. 1999. Interactions between mitogenic stimuli, or, a thousand and one connections. *Curr. Opin. Cell Biol.* 11:197–202.

Smith, M.W., M.A. Peacock, and E.K. Lund. 1986. Testing the hypothesis that crypt size determines the rate of enterocyte development in neonatal mice. *Comp. Biochem. Physiol. A.* 84:511–515.

Stallmach, A., B. von Lampe, H. Matthes, G. Bornhoft, and E.O. Riecken. 1992. Diminished expression of integrin adhesion molecules on human colonic epithelial cells during the benign to malign tumour transformation. *Gut.* 33:342–346.

Stallmach, A., B. von Lampe, H.D. Orzechowski, H. Matthes, and E.O. Riecken. 1994. Increased fibronectin-receptor expression in colon carcinoma-derived HT 29 cells decreases tumorigenicity in nude mice. *Gastroenterology.* 106:19–27.

Strater, J., U. Wedding, T.F. Barth, K. Koretz, C. Elsing, and P. Moller. 1996. Rapid onset of apoptosis in vitro follows disruption of beta 1-integrin/matrix interactions in human colonic crypt cells. *Gastroenterology.* 110:1776–1784.

van den Brink, G.R., S.A. Bleuming, J.C. Hardwick, B.L. Schepman, G.J. Offerhaus, J.J. Keller, C. Nielsen, W. Gaffield, S.J. van Deventer, D.J. Roberts, and M.P. Peppelenbosch. 2004. Indian Hedgehog is an antagonist of Wnt signaling in colonic epithelial cell differentiation. *Nat. Genet.* 36:277–282.

Varner, J.A., D.A. Emerson, and R.L. Juliano. 1995. Integrin alpha 5 beta 1 expression negatively regulates cell growth: reversal by attachment to fibronectin. *Mol. Biol. Cell.* 6:725–740.

Wang, L.C., F. Nassir, Z.Y. Liu, L. Ling, F. Kuo, T. Crowell, D. Olson, N.O. Davidson, and L.C. Burkly. 2002. Disruption of hedgehog signaling reveals a novel role in intestinal morphogenesis and intestinal-specific lipid metabolism in mice. *Gastroenterology.* 122:469–482.

Wary, K.K., F. Mainiero, S.J. Isakoff, E.E. Marcantonio, and F.G. Giancotti. 1996. The adaptor protein Shc couples a class of integrins to the control of cell cycle progression. *Cell.* 87:733–743.

Wary, K.K., A. Mariotti, C. Zurzolo, and F.G. Giancotti. 1998. A requirement for caveolin-1 and associated kinase Fyn in integrin signaling and anchorage-dependent cell growth. *Cell.* 94:625–634.

Whitehead, R.H., A. Brown, and P.S. Bhathal. 1987. A method for the isolation and culture of human colonic crypts in collagen gels. *In Vitro Cell. Dev. Biol.* 23:436–442.

Wong, M.H., J. Huelsken, W. Birchmeier, and J.I. Gordon. 2002. Selection of multipotent stem cells during morphogenesis of small intestinal crypts of Lieberkuhn is perturbed by stimulation of Lef-1/beta-catenin signaling. *J. Biol. Chem.* 277:15843–15850.

Woodford-Richens, K., J. Williamson, S. Bevan, J. Young, B. Leggett, I. Frayling, Y. Thway, S. Hodgson, J.C. Kim, T. Iwama, et al. 2000. Allelic loss at SMAD4 in polyps from juvenile polyposis patients and use of fluorescence in situ hybridization to demonstrate clonal origin of the epithelium. *Cancer Res.* 60:2477–2482.

Zhou, X.P., K. Woodford-Richens, R. Lehtonen, K. Kurose, M. Aldred, H. Hampel, V. Launonen, S. Virta, R. Pilarski, R. Salovaara, et al. 2001. Germline mutations in BMPR1A/ALK3 cause a subset of cases of juvenile polyposis syndrome and of Cowden and Bannayan-Riley-Ruvalcaba syndromes. *Am. J. Hum. Genet.* 69:704–711.

Zhu, X., and R.K. Assoian. 1995. Integrin-dependent activation of MAP kinase: a link to shape-dependent cell proliferation. *Mol. Biol. Cell.* 6:273–282. (published erratum appears in *Mol. Biol. Cell.* 1996. 7:1001)